Dynamic structure of strongly coupled one-component plasmas

Jongbae Hong and Cheolkyu Kim
Department of Physics Education, Seoul National University, Seoul, 151-742 Korea
(Received 13 August 1990; revised manuscript received 17 October 1990)

We study the dynamic behavior of the strongly coupled one-component classical plasmas by calculating a dynamic structure factor for various coupling strengths and momentum transfers in terms of the dynamically convergent calculation method recently developed. It is shown that the dynamically convergent calculation yields fast convergence, especially at large momentum transfer. We analyze the molecular-dynamics data for an intermediate momentum transfer at which the origin of the peak of power spectrum may be unclear, and show which elementary excitation is responsible for the peak. Our analysis also shows the disappearing process of plasma oscillation.

I. INTRODUCTION

The classical one-component plasma (OCP) that consists of homogeneous charged particles with neutralizing background has been thought of as a good nontrivial model to study classical many-body correlation effects.[1] It has been believed that the strongly coupled classical OCP exists only outside the Earth in places such as the interior of highly developed stars like white dwarfs, or the center of Jupiter.[2] For this reason, experimental data for this system can only be obtained through computer simulation. Recent experimental developments, however, indicate that the strongly coupled classical OCP may be realized in the laboratory in the near future.[3] Therefore it becomes more practical to study this system. The strength of coupling is expressed by a parameter $\Gamma=Ze^2/ak_BT$, where Z, k_B, and a are the atomic number, the Boltzmann constant, and the average radius of the ion, respectively. The strong and weak couplings are divided at $\Gamma=1$.

There are many interesting studies of this system made via a computer. The pair correlation function and the static structure factor have been obtained by Monte Carlo simulation[4] and other numerical calculations such as by solving the hypernetted chain equation.[5] In many cases, one is also interested in dynamical properties. The dynamical property of a many-body system is usually studied through the dynamic-structure factor which is a Fourier transform of the time autocorrelation function of the density fluctuation operator and is proportional to the inelastic scattering cross section. The dynamic-structure factors through molecular dynamics have been given by Hansen *et al.*[6] A number of theoretical works[7–9] to explain the computer experiments have been undertaken. But most of them introduce an appropriate damping function or memory function to explain the broadening phenomenon and the fine structure of the power spectrum. One of the typical dynamical theories in this field is the linear response theory,[10] in which the dynamic response function $\chi(k,\omega)$ is an essential quantity for describing the dynamical behavior of many-body systems. The fluctuation-dissipation theorem links theory and experiment by relating the imaginary part of $\chi(k,\omega)$ and the dynamic-structure factor, which is directly proportional to an inelastic scattering cross section measured by experiment.

It is usual to express the dynamic response function in terms of the dynamic local-field correction, for example, as

$$\chi(k,\omega)=\frac{\chi^0(k,\omega)}{1-v(k)[1-G(k,\omega)]\chi^0(k,\omega)}\ , \tag{1}$$

where $\chi^0(k,\omega)$ is the response function for the noninteracting system known as the Vlasov function,[11] $v(k)$ the Fourier transform of the interaction given by $4\pi(Ze)^2/k^2$ for Coulomb interaction, and $G(k,\omega)$ the so-called dynamical local-field correction. The variables k and ω mean transferred momentum and energy, respectively, during inelastic scattering between system and probing particle.

It is well known that in the dynamical theory the dynamic property, especially at intermediate momentum transfer, can never be fully understood by the static approximation $G(k,\omega)=G(k)$.[12] Therefore a correct frequency dependence in $G(k,\omega)$ is needed for an understanding of many-body dynamics. There have been several theories[13–15] providing analytic forms of $G(k,\omega)$ for quantum electron liquids. But no theory can explain satisfactorily the dynamic properties of a quantum electron liquid at intermediate momentum transfer where plasmon mode and single-particle excitation mode compete with each other and the multiple-particle excitation mode may not be negligible.

The classical OCP, on the other hand, has not been studied as much as its quantum-mechanical counterpart. An early attempt using the linear response theory for the classical OCP has been given by Kugler,[8] and a recent work considering dynamic local-field correction by Tanaka and Ichimaru[9] in their viscoelastic formalism. But they did not illustrate $G(k,\omega)$ explicitly. In this work, we calculate the dynamic local-field corrections in terms of the so-called dynamically convergent calculation method developed recently by Hong and Lee.[15] This first-principles method, of course, does not contain any assumption or undefined parameter, and the approximation process is so systematic that it gives more precise

$G(k,\omega)$ as the order of approximation increases. In our formalism, the static approximation $G(k,\omega)=G(k)$ is just our first-order approximation, and the frequency dependence in the local-field correction appears from the second-order approximation. The first-order approximation $G(k,\omega)=G(k)$ does not explain the power spectrum appropriately except for the case of small momentum transfer at which only the plasmon peak appears prominently. Therefore the frequency dependence in the local-field correction is crucial to an understanding of the fine structure of the power spectrum. We show the frequency-dependent local-field correction explicitly and calculate the dynamic-structure factor in terms of the local-field correction obtained by our method.

Most theoretical results for studying dynamic structure of OCP would be compared with the results obtained through molecular dynamics.[6] One can hardly understand the data by computer experiment without theoretical explanation. Especially at intermediate momentum transfers, the character of the peak in power spectrum may be unclear. It may not be simple to decide whether the peak is a decaying plasmon mode or a rising single-particle excitation mode. In our analysis, we will show that a misunderstanding could be possible if only first-order approximation is adopted. We will also analyze molecular-dynamics data in terms of the dynamically convergent calculation method by which the process of decaying plasmon and rising single-particle excitations is seen clearly.

This paper is composed of four sections. We introduce an exact formalism and systematic approximation for the dynamic local-field correction through the recurrence relation method[16] in Sec. II. In Sec. III, our formalism is applied to the classical OCP and the dynamic-structure factors are obtained. Comparison with molecular-dynamics data and their analysis is performed there. We give some discussions in Sec. IV.

II. EXACT FORMALISM AND APPROXIMATION

It is natural to choose the density fluctuation operator ρ_k for a dynamical variable to study the dynamic properties of a homogeneous many-particle system. The dynamic properties we want to know in this work may be given by solving the generalized Langevin equation derived first by Mori[17] and later more easily by the recurrence relation method[16] in a dynamical Hilbert space defined by the Kubo scalar product[16,17] as an inner product. The slowly varying linear part of the solution of the generalized Langevin equation for ρ_k in the above Hilbert space is called the relaxation function and is related to the density-response function (1). Therefore the latter function is a fundamental quantity in the dynamical theory of linear response.

Since we are interested in linear response of the system, calculating response function (1) is sufficient for this work. To obtain the response function, we need to know $\chi^0(k,\omega)$ and $G(k,\omega)$. General classical noninteracting response functions given by Vlasov[11] such as

$$\chi^0(k,\omega)=-\frac{n}{k_BT}W(x)\ , \tag{2}$$

where

$$W(x)=1-xe^{-(1/2)x^2}\times\int_0^x dy\left[\exp\left[\frac{y^2}{2}\right]+ix\left[\frac{\pi}{2}\right]^{1/2}\exp\left[-\frac{x^2}{2}\right]\right],$$

$x=(\omega/k)(m/k_BT)^{1/2}$, and n and m are density and particle mass, respectively, can be used for the classical OCP. Since $v(k)=4\pi(Ze)^2/k^2$, the remaining effort for obtaining $\chi(k,\omega)$ is to calculate the dynamic local-field correction $G(k,\omega)$. We show in what follows the expressions of $G(k,\omega)$ in systematically approximated forms through the dynamically convergent calculation method.[15]

The dynamically convergent calculation method is constructed by using the recurrence relation method[16] as follows. Let A by a dynamical variable whose time evolution is required to understand the dynamics of a system under consideration. The time evolution $A(t)$ may be expanded in terms of orthogonal bases $\{f_\nu,\ \nu=0,1,2,\ldots,D-1\}$ spanning a D-dimensional dynamical Hilbert space, i.e., $A(t)=\sum_{\nu=0}^{D-1}a_\nu(t)f_\nu$. The inner product of this Hilbert space is defined as $(X,Y)=\langle XY^*\rangle$, where $\langle\ \rangle$ and the asterisk mean the classical ensemble average and complex conjugate, respectively, and X,Y are elements of the Hilbert space. The inner product is just the classical form of the Kubo scalar product.

If we set $f_0=A$ and take orthogonalization process in terms of the property $(\dot X,Y)=-(X,\dot Y)$, the following recurrence relation[16,18] for f_ν is obtained:

$$f_{\nu+1}=\dot f_\nu+\Delta_\nu f_{\nu-1} \tag{3}$$

where $\Delta_\nu=(f_\nu,f_\nu)/(f_{\nu-1},f_{\nu-1})$, $f_{-1}\equiv0$, and $\dot f_\nu=\{H,f_\nu\}_{\rm PB}$, H is the Hamiltonian. Here $\{\ ,\ \}_{\rm PB}$ represents the Poisson bracket. Another recurrence relation[16] for the coefficients $a_\nu(t)$ of Eq. (2) can be obtained by substituting (3) into (2), i.e.,

$$\Delta_{\nu+1}a_{\nu+1}(t)=-\dot a_\nu(t)+a_{\nu-1}(t)\ , \tag{4}$$

where $a_{-1}(t)\equiv0$. Laplace transform of Eq. (4) is written as

$$\Delta_1a_1(z)=1-za_0(z),\quad \nu=0\ , \tag{5}$$

$$\Delta_{\nu+1}a_{\nu+1}(z)=a_{\nu-1}(z)-za_\nu(z),\quad \nu\geq1\ . \tag{6}$$

The $a_0(z)=(A(z),A)/(A,A)=\langle A(z)A^*\rangle/\langle AA^*\rangle$ is the normalized Laplace transformed relaxation function of the dynamical variable A. The relaxation function in this paper appears as an autocorrelation function, because we treat the classical system. By choosing the density fluctuation $\rho_k=\sum_{i=1}^N\exp(-ikr_i)$ as a dynamical variable, one can relate $a_0(z)$ to the density-response function[15] such that

$$1-za_0(z)=\chi(k,z)/\chi(k)\ , \tag{7}$$

where $\chi(k)=\chi(k,0)$. The frequency-dependent response function is obtained by setting $z=i\omega+0^+$. Dividing Eqs. (5) and (6) by $a_0(z)$ and manipulating a little we have a continued fraction expression for $a_0(z)$ as

$$a_0(z)=\frac{1}{z+\Delta_1 b_1(z)} , \tag{8}$$

where

$$b_1(z)=\frac{1}{z+\Delta_2 c_2(z)} , \tag{9}$$

$$c_2(z)=\frac{1}{z+\Delta_3 d_3(z)} , \tag{10}$$

$$\vdots$$

Since $b_1(z)$ contains all Δ's except Δ_1 in the same manner as $a_0(z)$, it can be understood that $b_1(z)$ is the relaxation function of the random force f_1. Similarly, we get the same structure of continued fraction for $c_2(z)$, $d_3(z)$, etc. starting from Δ_3, Δ_4, etc., respectively. Therefore one understands that they are relaxation functions of higher-order random forces f_2, f_3, and so on. Combining (7) and (8), one obtains

$$\frac{\chi(k,z)}{\chi(k)}=\frac{\Delta_1 b_1(z)}{z+\Delta_1 b_1(z)} . \tag{11}$$

One can also imagine that the same form as (11) can be written for the noninteracting system as

$$\frac{\chi^0(k,z)}{\chi^0(k)}=\frac{\Delta_1^0 b_1^0(z)}{z+\Delta_1^0 b_1^0(z)} . \tag{12}$$

Dividing (12) by (13) and using the identity $\Delta_1^0/\Delta_1=\chi(k)/\chi^0(k)$ which comes from the property $f_1=\{H,\rho_k\}_{\rm PB}=\{H^0,\rho_k\}_{\rm PB}=f_1^0$ valid in this system, one gets the following form for $\chi(k,z)$:

$$\chi(k,z)=\frac{\chi^0(k,z)}{\frac{b_1^0(z)}{b_1(z)}\left[\frac{z+\Delta_1 b_1(z)}{z+\Delta_1^0 b_1^0(z)}\right]} . \tag{13}$$

If we set $\chi(k,z)\equiv\chi^0(k,z)/[1-\Lambda(z)\chi^0(k,z)]$ like Eq. (1), $\Lambda(z)$, compared with Eq. (13), is written as

$$\Lambda(z)=\frac{1}{\chi^0(k,z)}-\frac{b_1^0(z)}{b_1(z)}\left[\frac{z+\Delta_1 b_1(z)}{z+\Delta_1^0 b_1^0(z)}\right]\frac{1}{\chi^0(k,z)} . \tag{14}$$

Substituting (12) into (14), $\Lambda(z)$ is given by

$$\begin{aligned}\Lambda(z)&=[\chi^0(k)^{-1}-\chi(k)^{-1}]-\frac{z}{\chi^0(k)\Delta_1^0}[b_1(z)^{-1}-b_1^0(z)^{-1}]\\&=v(k)[1-G(k)]-\frac{z}{\chi^0(k)\Delta_1^0}[b_1(z)^{-1}-b_1^0(z)^{-1}] .\end{aligned} \tag{15}$$

Since $\Lambda(z)=v(k)[1-G(k,z)]$ from Eq. (1), the dynamic local-field correction is expressed as

$$G(k,z)=G(k)+\frac{z}{v(k)\chi^0(k)\Delta_1^0}[b_1(z)^{-1}-b_1^0(z)^{-1}] . \tag{16}$$

This is an exact formal expression for the dynamic local-field correction. We can write other expressions in terms of Eqs. (9), (10), etc. as

$$\begin{aligned}G(k,z)&=G(k)+\frac{z}{v(k)\chi^0(k)\Delta_1^0}[\Delta_2 c_2(z)-\Delta_2^0 c_2^0(z)] \qquad (17)\\&=G(k)+\frac{z}{v(k)\chi^0(k)\Delta_1^0}\times\left[\frac{\Delta_2}{z+\Delta_3 d_3(z)}-\frac{\Delta_2^0}{z+\Delta_3^0 d_3^0(z)}\right] . \qquad (18)\end{aligned}$$

The frequency-dependent local-field correction is given by taking $z=i\omega+0^+$. Up to now we did not make any approximation. But for practical applications we need to make approximations for random force correlation functions appearing in (16), (17), (18), etc.

The conventional approximation method in many-body theory is the random-phase approximation (RPA) which corresponds to setting $G(k,z)=0$. A little improved approximation is the static approximation, i.e., $G(k,z)=G(k)$, which corresponds to setting $b_1(z)=b_1^0(z)$ in Eq. (16), which we call the first-order approximation. For the quantum electron gas, the static results obtained by the static approximation[12] were reasonably good, but the application to studying dynamic behavior was not good enough to explain dynamic structure. We also show in this work that the static approximation cannot explain the dynamics of a strongly coupled system.

Our higher-order approximations are given by replacing the relaxation functions of higher-order random forces, $c_2(z)$, $d_3(z)$, etc., with their noninteracting counterparts, $c_2^0(z)$, $d_3^0(z)$, etc., respectively. Then we find the following approximated forms of the dynamic local-field correction:

$$G^{(1)}(k,\omega)=G(k) , \tag{19}$$

$$G^{(2)}(k,\omega)=G(k)+\frac{\eta_2 Q(k,\omega)}{v(k)\chi^0(k)} , \tag{20}$$

$$G^{(3)}(k,\omega)=G(k)+\frac{[\eta_2-\eta_3 R(k,\omega)]Q(k,\omega)}{v(k)\chi^0(k)[1+\eta_3 R(k,\omega)]} , \tag{21}$$

where $\eta_i=(\Delta_i/\Delta_i^0)-1$, $Q(k,\omega)=\chi^0(k)/\chi^0(k,\omega)+\omega^2/\Delta_1^0-1$, and $R(k,\omega)=1-\Delta_1^0 Q(k,\omega)/\Delta_2^0$. We will show in the following section that the frequency dependence in $G(k,\omega)$ plays a crucial role in describing the dynamic behaviors of the strongly coupled OCP.

III. STRONGLY COUPLED CLASSICAL OCP

Now we study the dynamic properties of the classical OCP through the method introduced in preceding sections. We take ρ_k as our dynamical variable, and define the inner product of the dynamical Hilbert space of ρ_k as a classical ensemble average of the product of a vector in the Hilbert space and its complex conjugate. Then we have the following set of orthogonal vectors spanning the Hilbert space from the recurrence relation (3) as $f_0=\rho_k$, $f_1=\dot\rho_k$, $f_2=\ddot\rho_k+\Delta_1\rho_k$, and so on. The Δ's are given by frequency moments;

$$\Delta_1=\frac{\langle f_1 f_1^* \rangle}{\langle f_0 f_0^* \rangle}=\frac{\langle \omega^2 \rangle}{\langle \omega^0 \rangle} , \tag{22}$$

$$\Delta_2=\frac{\langle f_2 f_2^* \rangle}{\langle f_1 f_1^* \rangle}=\frac{\langle \omega^4 \rangle}{\langle \omega^2 \rangle}-\frac{\langle \omega^2 \rangle}{\langle \omega^0 \rangle} , \tag{23}$$

$$\vdots$$

where $\langle \omega^{2n} \rangle \equiv \langle \rho_k^{(n)} (\rho_k^{(n)})^* \rangle$ means $2n$th frequency moment.

According to the dynamical theory of the preceding section, we are required to know some static information such as η_i and $G(k)$ before performing dynamic calculation. So we calculate Δ's first, since $\eta_i=(\Delta_i/\Delta_i^{(0)})-1$. The Δ's are given by Eqs. (22) and (23) in terms of frequency moments. The zeroth moment $\langle \rho_k \rho_k^* \rangle$ is just the negative static susceptibility whose noninteracting expression is $-\chi^0(k)=n/k_B T$. The second and fourth moment are easily allowed.[19] They are written, respectively, as

$$\langle \omega^2 \rangle=\frac{n}{k_B T}\frac{\omega_p^2 k^2}{3\Gamma} , \tag{24}$$

$$\langle \omega^4 \rangle=\frac{n}{k_B T}\frac{\omega_p^4 k^2}{3\Gamma}\left[1+\frac{k^2}{\Gamma}+\frac{1}{N}\sum_{\mathbf{p}}\frac{(\mathbf{p}\cdot\mathbf{k})^2}{k^2 p^2}[S(\mathbf{p}-\mathbf{k})-S(\mathbf{p})]\right]$$

$$=\frac{n}{k_B T}\frac{\omega_p^4 k^2}{3\Gamma}\left[1+\frac{k^2}{\Gamma}-I(k)\right] \tag{25}$$

where

$$I(k)=\frac{1}{3\pi}\int_0^\infty dp\, p^2[1-S(p)]\times\left[\frac{5}{6}-\frac{p^2}{2k^2}+\frac{(k^2-p^2)^2}{4pk^3}\ln\left|\frac{p+k}{p-k}\right|\right] , \tag{26}$$

$\omega_p=(4\pi n e^2/m)^{1/2}$, the plasma frequency, and we set $Z=1$ for convenience. The noninteracting counterparts of Eqs. (24) and (25) are $\langle \omega^2 \rangle^0=(n/k_B T)(\omega_p^2 k^2/3\Gamma)$ and $\langle \omega^4 \rangle^0=(n/k_B T)(\omega_p^4 k^4/3\Gamma^2)$.

Thus the Δ's and Δ^0's are given, respectively, by $\Delta_1=\omega_p^2[1-G(k)]+\omega_p^2 k^2/3\Gamma$, $\Delta_1^0=\omega_p^2 k^2/3\Gamma$, and $\Delta_2=2\omega_p^2 k^2/3\Gamma-\omega_p^2 I(k)+\omega_p^2 G(k)$, $\Delta_2^0=2\omega_p^2 k^2/3\Gamma$. Then we can find $\eta_2=\Delta_2/\Delta_2^0-1=(3\Gamma/2k^2)[G(k)-I(k)]$.

There is an exact relationship between $G(k)$ and the structure factor $S(k)$ for a classical many-body system[20] such as

$$G(k)=1+\left[1-\frac{1}{S(k)}\right]\frac{k^2}{3\Gamma} . \tag{27}$$

Using this relation and Eq. (26), the η_2 is given by the static structure factor only, i.e.,

$$\eta_2=\frac{3\Gamma}{2k^2}[1-I(k)]+\frac{1}{2}\left[1-\frac{1}{S(k)}\right] . \tag{28}$$

Hence if we have the static structure factor $S(k)$, our first- and second-order approximations will be followed. In this work, however, we do not perform static calculations to get $S(k)$ and $I(k)$. Instead, we will borrow the data obtained by Monte Carlo method by Hansen.[21] To ge the third-order approximation (22), we need a sixth frequency moment $\langle \omega^6 \rangle$ to obtain η_3, the precise value of which is not easy to evaluate, because it contains three-body correlation. To our knowledge there is no reliable calculation treating three-body correlation. Therefore we use η_3 as a parameter to see the effects of our third-order approximation. One can imagine that the three-body correlation does not play an important role in the case of large momentum transfer. Therefore the second order may be enough for the case. We will verify this later.

Having this static information, it is straightforward to get dynamic local-field corrections and dynamic-structure factors up to third order for a chosen Γ and momentum transfer. To make things easier, we reexpress given formulas in terms of dimensionless variables so that wave vector k and frequency ω are in units of inverse ion radius a^{-1}, $a^3=3/4\pi n$, and plasma frequency ω_p, respectively. Then the argument x in the Vlasov function (2) is represented by $x=[(3\Gamma)^{1/2}/k]\omega$. The dynamic local-field corrections in (20) and (21) are also rewritten as

$$G^{(2)}(k,\omega)=G(k)-\frac{\eta_2 k^2}{3\Gamma}Q(k,\omega) , \tag{29}$$

$$G^{(3)}(k,\omega)=G(k)-\frac{k^2}{3\Gamma}\frac{[\eta_2-\eta_3 R(k,\omega)]Q(k,\omega)}{1+\eta_3 R(k,\omega)} , \tag{30}$$

where $Q(k,\omega)=1/W(x)+x^2-1$ and $R(k,\omega)=1-\frac{1}{2}Q(k,\omega)$. The dynamic-structure factor, defined by $S(k,\omega)=-(k_B T/n\pi\omega)\mathrm{Im}\chi(k,\omega)$ for the classical case, is given by

$$S(k,\omega)=\frac{1}{\pi\omega}\mathrm{Im}\frac{W(x)}{1+(3\Gamma/k^2)W(x)[1-G(k,\omega)]} . \tag{31}$$

Now we are in a position to compare molecular-dynamics data[6] with our theory. For a meaningful comparison, we fix momentum transfer at $k=6.187$, which corresponds to comparatively large momentum transfer, then select various coupling strengths such as $\Gamma=152.4$, 110.4, and 9.7. For each case, corresponding $G(k)$ are 0.9273, 0.9308, and 1.0046 and η_2 are 1.9250, 1.3790, and 0.1226, respectively. These values are given by using Eqs. (27) and (28), and the results for $S(k)$ and $I(k)$ in Ref. 6(b). We show the first- and second-order graphs of $S(k,\omega)$ for these cases in Fig. 1 with graphs of RPA corresponding to $G(k,\omega)=0$, and compare with data obtained by molecular dynamics.[6] We do not need third order in these cases, because the approximation gives fast convergence. Let us look at the case $\Gamma=152.4$, for example; the RPA and the first order still have a prominent plasmon peak which should be damped off completely at this large momentum transfer as molecular-dynamics data show. But the second order which includes the frequency dependence in $G(k,\omega)$ causes a drastic change in dynamic form factors, and the collective mode, in this order, nearly fades away. That means our approximation process is very effective for a large momentum transfer.

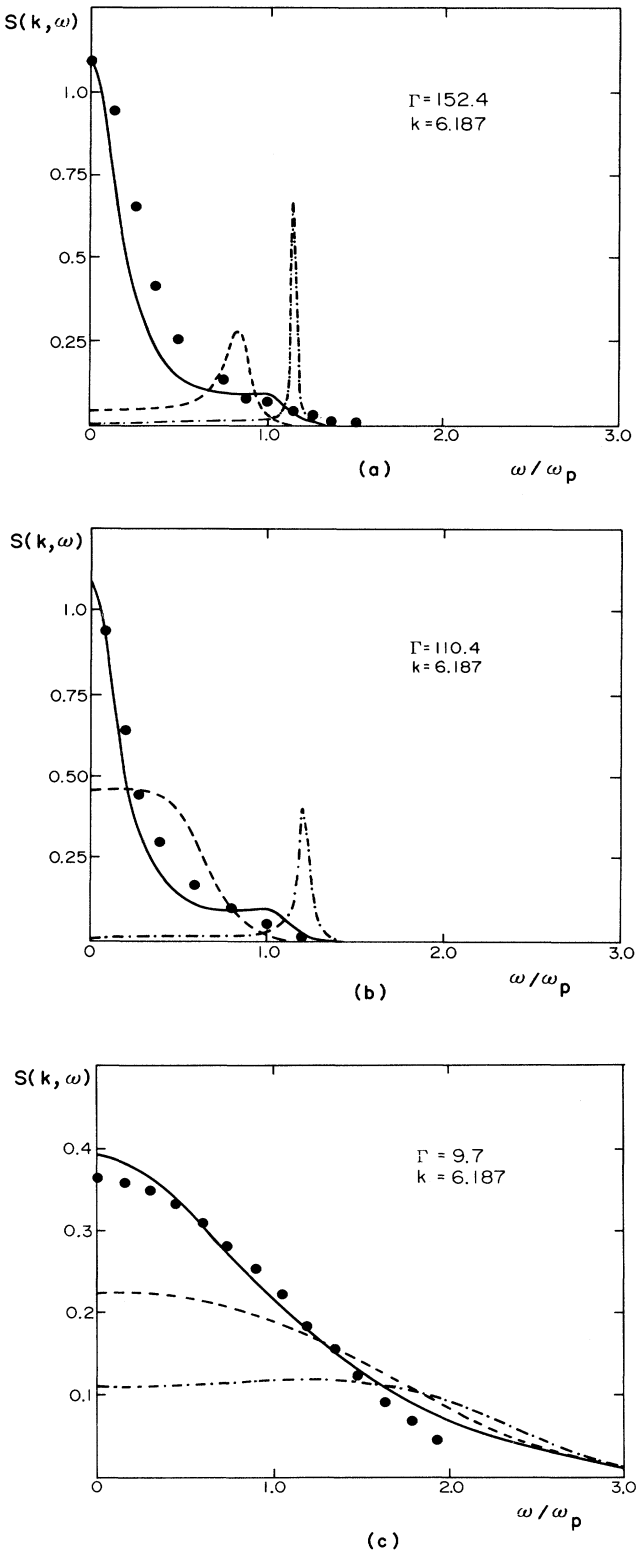

FIG. 1. Dynamic-structure factors for (a) $\Gamma=152.4$, $G(k)=0.9273$, $\eta_2=1.7950$; (b) $\Gamma=110.4$, $G(k)=0.9308$, $\eta_2=1.3790$; (c) $\Gamma=9.7$, $G(k)=1.0046$, $\eta_2=0.1226$. For each Γ, $k=6.187$. Dash-dotted line is RPA, dashed line, first order, solid line, second order, and black dots are molecular-dynamics data.

The high peak at $\omega=0$ in Fig. 1 stems from single-particle excitations. One can also see that as the coupling strength becomes weaker, even the first-order graph in $\Gamma=9.7$ approaches reasonable values. Therefore we can insist that our approximation become more effective for small Γ and large k.

As a second example, we choose an intermediate momentum transfer $k=2.315$ for a system $\Gamma=9.7$. For this case $G(k)=0.5334$ and $\eta_2=0.5685$. At this intermediate momentum transfer, the second-order graph is still unsatisfactory as shown in Fig. 2. The third order, therefore, is indispensable to explain the structure of data given by molecular dynamics correctly. Since a numerical value of η_3 is not available from any static calculation, we use η_3 as a parameter. We vary η_3 slowly from zero and find a reasonable value $\eta_3=0.6522$ at which the third-order graph becomes the best shape. If η_3 is larger than this value, the graph tends to deviate quite a lot from the data. Figure 2 contains each approximation order and RPA graph to compare with molecular-dynamics data. In the figure, the first-order graph seems to be good. But it leads to a misunderstanding, since the peaks in the data and the first-order approximation have totally different origins. This fact becomes clear if we go to higher orders. Though the second order looks pretty bad, it imposes important physical meanings showing the degeneration of the plasmon peak and the generation of a new peak which is caused by single-particle excitations. The second order is considered as an intermediate step approaching a real situation. One may conclude from Fig. 2 that the plasmon peak appearing in the RPA graph is damped off and only a small remnant of the collective mode remains around $\omega=1.5\omega_p$, and the main peak is transported from $\omega=0$ side at which the single-particle excitations make a broad peak at large k.

In conclusion, our dynamically convergent calculation

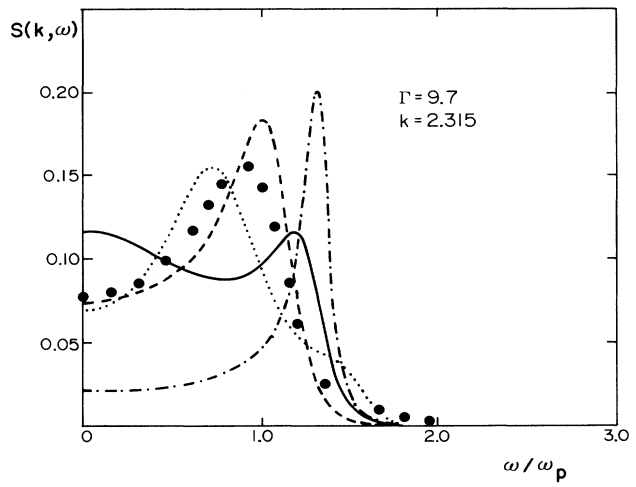

FIG. 2. Dynamic-structure factor for $\Gamma=9.7$ and $k=2.315$. Here $G(k)=0.5334$, $\eta_2=0.5685$, and $\eta_3=0.6522$. Dash-dotted line is RPA, dashed line, first order, solid line, second order, and dotted line, third order. Black dots are molecular-dynamics data.

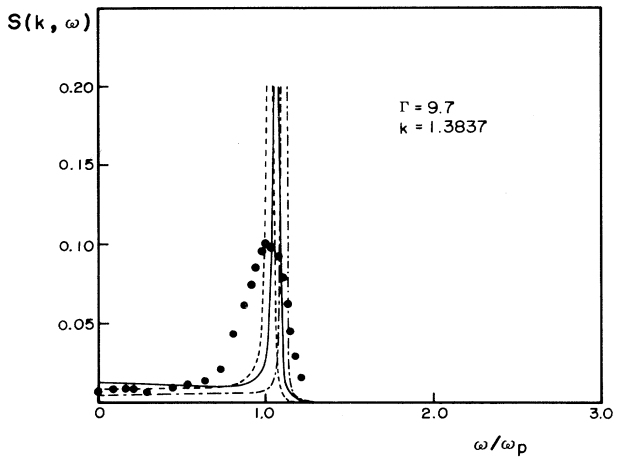

FIG. 3. Dynamic-structure factor for $\Gamma=9.7$ and $k=1.3837$. Here $G(k)=0.1955$ and $\eta_2=0.5084$. Dash-dotted line is RPA, dashed line, first order and solid line, second order.

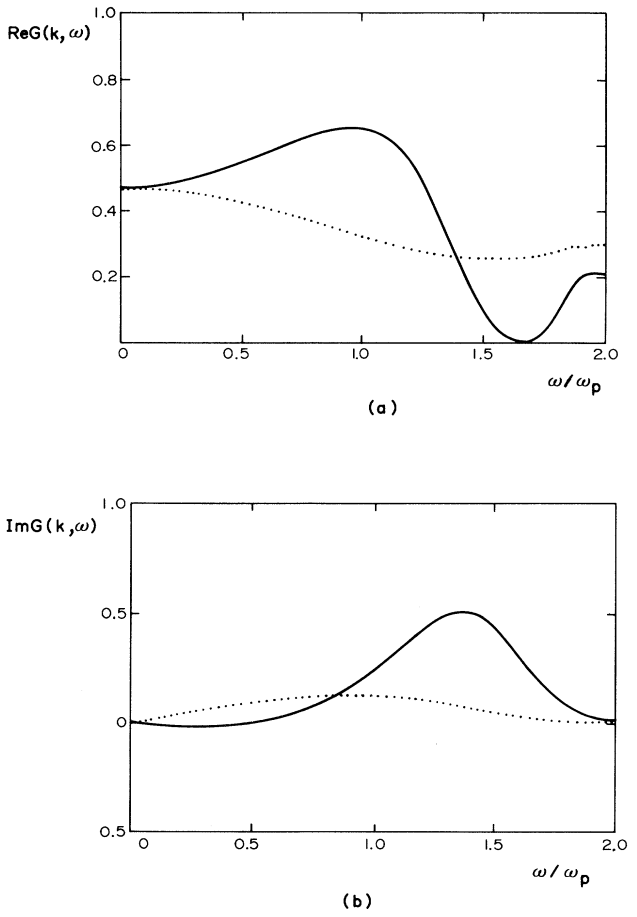

FIG. 4. (a) Real part and (b) imaginary part of dynamic local-field correction for $\Gamma=9.7$ and $k=2.315$. Dotted lines mean second order and solid lines third order.

method provides us with a clear understanding of the dynamic structure of the strongly coupled classical OCP. We also studied the small momentum transfer case in which the molecular-dynamics data show a single plasmon peak near plasma frequency with some width. Theoretical dynamic-structure factors obtained by the present method and even RPA show very sharp peaks near plasma frequency. No discernible difference is seen among them. We illustrate this property for $k=1.3837$ and $\Gamma=9.7$ in Fig. 3. One can see that the positions of the plasmon peak are nearly the same. Therefore we can say that our approximation scheme is not that useful at low k regime because even RPA is very good at the regime. Since the dynamic local-field correction, on the other hand, has never been plotted for the classical OCP as far as we know, it is interesting to plot the real and imaginary parts of $G(k,\omega)$. For this reason, we plot real and imaginary parts of $G(k,\omega)$ for $k=2.315$ and $\Gamma=9.7$, for instance, in Fig. 4.

IV. DISCUSSION

The method used in this work is the classical version of quantum-mechanical theory[15] which has been applied to the electron gas at metallic density. The correct frequency moments are the only necessary static information to study dynamic properties in applying this method. The zeroth moment, the negative static susceptibility, contains the static local-field correction $G(k)$ as an unknown quantity, but fortunately there is a nice relationship between the static structure factor $S(k)$ and the $G(k)$ for the classical systems. For quantum systems, however, this is not the case. On the other hand, since the second frequency moment is easily given for a system having velocity-independent potential[22] and the fourth frequency moment is given by a functional form of $S(k)$, the static structure factor which describes two-body correlation, therefore, gives rise to the correct zeroth, second, and fourth frequency moments. Thus our approximation process can reach to the second order in terms of given $S(k)$.

The difficulty arises in calculating the sixth frequency moment[23] in which three-body correlations are involved. Unfortunately, there is no information about static correlations for more than two bodies. For large momentum transfer, nevertheless, the three-body correlation effects could be neglected, since the scattering time may be very short. Thus our second-order approximation is enough to yield very good agreements with molecular-dynamics data at large k. As we saw in the preceding section, only intermediate momentum transfer requires higher-order approximation. But the convergence of our method is very fast so that only third order may be enough to describe dynamic behaviors of the system.

ACKNOWLEDGMENTS

This work has been supported by the Seoul National University Daewoo Research Fund.

[1]S. Ichimaru, Rev. Mod. Phys. **54**, 1017 (1982); M. Baus and J.-P. Hansen, Phys. Rep. **59**, 1 (1980).

[2]See *Strongly Coupled Plasmas,* edited by G. Kalman and P. Carini (Plenum, New York, 1978).

[3]J. J. Bollinger and D. J. Wineland, Phys. Rev. Lett. **53**, 348 (1984); C. F. Driscoll and J. H. Malmberg, *ibid.* **50**, 167 (1983).

[4]J.-P. Hansen, Phys. Rev. A **8**, 3096 (1973); W. L. Slattery, G. D. Doolen, and H. E. DeWitt, *ibid.* **21**, 2087 (1980); **26**, 2255 (1982); S. G. Brush, H. L. Sahlin, and E. Teller, J. Chem. Phys. **45**, 2102 (1966).

[5]J. F. Springer, M. A. Pokrant, and F. A. Stevens, J. Chem. Phys. **58**, 4863 (1973); K. C. Ng, *ibid.* **61**, 2680 (1974).

[6](a) J.-P. Hansen, E. L. Pollack, and I. R. McDonald, Phys. Rev. Lett. **32**, 277 (1974); (b) Phys. Rev. A **11**, 1025 (1975).

[7]S. K. Mitra and S. Sjodin, J. Phys. C **11**, 2655 (1978); J. Bosse and K. Kubo, Phys. Rev. A **18**, 2337 (1978); R. Cauble and J. J. Duderstadt, *ibid.* **23**, 3182 (1981).

[8]A. A. Kugler, J. Stat. Phys. **8**, 107 (1973).

[9]S. Ichimaru and S. Tanaka, Phys. Rev. Lett. **56**, 2815 (1986); S. Tanaka and S. Ichimara, Phys. Rev. A **35**, 4743 (1987).

[10]R. Kubo, J. Phys. Soc. Jpn. **12**, 570 (1957).

[11]A. A. Vlasov, Zh. Eksp. Teor. Fiz. **8**, 291 (1938) [Sov. Phys.—Usp. **10**, 721 (1968)]; see also Ref. 21.

[12]K. S. Singwi, M. P. Tosi, R. H. Land, and A. Sjolander, Phys. Rev. **176**, 589 (1968); P. Vashishta and K. S. Singwi, Phys. Rev. B **6**, 875 (1972); K. N. Pathak and P. Vashishta, *ibid.* **7**, 3647 (1973).

[13]A. Holas, P. K. Aravind, and K. S. Singwi, Phys. Rev. B **20**, 4912 (1979); P. K. Aravind, A. Holas, and K. S. Singwi, *ibid.* **25**, 561 (1982).

[14]J. T. Devreese, F. Brosens, and L. F. Lemmens, Phys. Rev. B **21**, 1349 (1980); **21**, 1363 (1980).

[15]J. Hong and M. H. Lee, Phys. Rev. Lett. **55**, 2375 (1985).

[16]M. H. Lee, J. Math. Phys. **24**, 2512 (1983); Phys. Rev. B **26**, 2547 (1982).

[17]H. Mori, Prog. Theor. Phys. **33**, 423 (1965).

[18]M. Dupuis, Prog. Theor. Phys. **37**, 502 (1967).

[19]D. Forster, P. C. Martin, and S. Yip, Phys. Rev. **170**, 160 (1968); see also Ref. 7(b).

[20]S. Ichimaru, *Basic Principles of Plasma Physics* (Benjamin, Reading, MA, 1973).

[21]Note that our $I(k)$ is two times larger than $I(k)$ of Ref. 7(b).

[22]D. Pines and P. Nozières, *Theory of Quantum Liquids* (Benjamin, New York, 1966).

[23]P. Vieillefosse and J.-P. Hansen, Phys. Rev. A **12**, 1106 (1975); S. Ichimaru, T. Tange, and D. Pines, Prog. Theor. Phys. **54**, 1077 (1975).